Asymmetries at e^+e^- colliders from E_6 grand unified theories

G. Bélanger and Stephen Godfrey
TRIUMF, 4004 Wesbrook Mall, Vancouver, British Columbia, Canada V6T 2A3
(Received 13 March 1986; revised manuscript received 28 July 1986)

Motivated by the resurgence of interest in E_6 grand unified theories due to their possible relevance as the low-energy limit of superstring theories, we studied the effects of the extra Z^0 bosons predicted by these theories on asymmetries in e^+e^- collisions. It was found that the deviations from the standard model allowed by low-energy phenomenology can be quite substantial and that asymmetries at e^+e^- colliders offer a sensitive probe for new physics. We describe a method of unraveling the underlying physics from the experimental data.

I. INTRODUCTION

Recently, there has been a resurgence of interest in E_6 grand unified theories (GUT's) motivated by the possibility that they represent the low-energy limit of superstring theories.[1] Because in superstring theories E_6 is broken by a discrete symmetry to a rank-5 or -6 group, one feature, common to all low-energy limits of this theory, is the prediction of at least one extra neutral gauge boson with the properties of the extra Z^0 bosons and their couplings to fermions dependent on the details of the symmetry breaking.[2] In this context, various aspects of E_6 GUT's have recently been studied: allowed symmetry-breaking patterns,[3] properties of extra fermions in E_6 (Refs. 4 and 5), and the properties and constraints on extra neutral gauge bosons. For the latter, several groups have examined the constraints that low-energy neutral-current data can put on the properties of the extra Z^0 bosons.[6,7] Beyond this, one may ask, how might these extra Z^0's, which we will refer to as Z''s, manifest themselves in the next generation of experiments and how might we unravel their properties. In order to answer these questions we have studied the effects of the extra Z^0's of E_6 in e^+e^- collisions. Specifically, we have examined the forward-backward asymmetries and the left-right asymmetries that arise from an initially polarized e^- beam and compared them to the asymmetries expected from the standard model.[8]

We begin in Sec. II with a brief overview of the relevant group theory necessary for the calculation of the extra Z^0 couplings to fermions. In Sec. III we present the formulas for the cross sections and asymmetries for polarized electron beams along with results for various values of the Z' mass, its couplings to fermions, and allowed values for Z^0-Z' mixing. We conclude with a description of how the underlying physics can be unraveled from the measured asymmetries along with some comments.

II. GROUP-THEORETICAL CONSIDERATIONS

Since E_6 is a rank-6 group it has six diagonal generators in its Cartan subalgebra which correspond to the axes of the six-dimensional root space.[9,10] At low energy E_6 must contain, at the least, the $SU(3)_C \times SU(2)_L \times U(1)$ symmetry of the standard model, so two of the diagonal generators are accounted for by the diagonal generators of $SU(3)_C$ and two other directions in the group space correspond to the photon and the Z^0 gauge boson. This leaves two remaining directions of E_6 group space available for new physics and, hence, extra Z^0 bosons. In principle, the extra Z^0 bosons can mix with the standard model Z^0 with the mixing angles constrained by experiment. We postpone a discussion of mixing effects for now and assume that the Z^0 couples as in the standard model to $I_{3L} - Q_{\rm EM}\sin^2\theta_W$. Since the charge of the extra Z^0 bosons, Q' and Q'', must be orthogonal to all generators of the standard model we can label the extra Z^0 charges using $U(1)_\chi$ and $U(1)_\psi$ which come from the subgroup chain:

$$E_6 \rightarrow SO(10) \times U(1)_\psi \rightarrow SU(5) \times U(1)_\chi \times U(1)_\psi \,. \tag{1}$$

Therefore, the charges Q' and Q'' will be given by any linear combination of the generators $U(1)_\chi$ and $U(1)_\psi$ with respective charges Q_χ and Q_ψ giving

$$Q' = Q_\chi \cos\theta_{E_6} + Q_\psi \sin\theta_{E_6} \,, \tag{2a}$$

$$Q'' = -Q_\chi \sin\theta_{E_6} + Q_\psi \cos\theta_{E_6} \,. \tag{2b}$$

Specific choices of θ_{E_6} correspond to different symmetry-breaking patterns which can be related to different subgroup chains. As an example, consider the case where E_6 is broken via a non-Abelian discrete symmetry to a rank-5 group:[5]

$$E_6 \rightarrow SU(3)_C \times SU(2)_L \times U(1)_L \times U(1) \,, \tag{3}$$

where the generator of U(1) is $I_{3R} + Y_R/2$, $I_{3L(R)}$ are generators of $SU(2)_{L(R)}$, and $Y_{L(R)}$ are generators of $U(1)_{L(R)}$ for the following subgroup chain:

$$E_6 \rightarrow SU(3)_C \times SU(3)_L \times SU(3)_R \,,$$

with

$$SU(3)_L \rightarrow SU(2)_L \times U(1)_L \tag{4}$$

and

$$SU(3)_R \rightarrow SU(2)_R \times U(1)_R \,.$$

TABLE I. Charges and quantum numbers of the left-handed fermions of the fundamental 27 representation in E_6.

	Q	I_{3L}	I_{3R}	Y_L	Y_R	$2\sqrt{10}Q_\chi$	$\sqrt{24}Q_\psi$	$2\sqrt{15}Q_\eta$
e^+	1	0	$\frac{1}{2}$	$\frac{2}{3}$	$\frac{1}{3}$	-1	1	-2
d	$-\frac{1}{3}$	$-\frac{1}{2}$	0	$\frac{1}{3}$	0	-1	1	-2
u	$\frac{2}{3}$	$\frac{1}{2}$	0	$\frac{1}{3}$	0	-1	1	-2
$\bar{u}$	$-\frac{2}{3}$	0	$-\frac{1}{2}$	0	$-\frac{1}{3}$	-1	1	-2
$\bar{d}$	$\frac{1}{3}$	0	$\frac{1}{2}$	0	$-\frac{1}{3}$	3	1	1
e^-	-1	$-\frac{1}{2}$	0	$-\frac{1}{3}$	$-\frac{2}{3}$	3	1	1
ν_e	0	$\frac{1}{2}$	0	$-\frac{1}{3}$	$-\frac{2}{3}$	3	1	1
$\bar{N}$	0	0	$-\frac{1}{2}$	$\frac{2}{3}$	$\frac{1}{3}$	-5	1	-5
$\bar{h}$	$\frac{1}{3}$	0	0	0	$\frac{2}{3}$	-2	-2	1
E^-	-1	$-\frac{1}{2}$	$-\frac{1}{2}$	$-\frac{1}{3}$	$\frac{1}{3}$	-2	-2	1
ν_E	0	$\frac{1}{2}$	$-\frac{1}{2}$	$-\frac{1}{3}$	$\frac{1}{3}$	-2	-2	1
h	$-\frac{1}{3}$	0	0	$-\frac{2}{3}$	0	2	-2	4
E^+	1	$\frac{1}{2}$	$\frac{1}{2}$	$-\frac{1}{3}$	$\frac{1}{3}$	2	-2	4
$\bar{N}_E$	0	$-\frac{1}{2}$	$\frac{1}{2}$	$-\frac{1}{3}$	$\frac{1}{3}$	2	-2	4
n	0	0	0	$\frac{2}{3}$	$-\frac{2}{3}$	0	4	-5

In this model the electromagnetic charge operator is given by

$$Q_{\rm EM}=I_{3L}+I_{3R}+\frac{Y_L+Y_R}{2} \tag{5}$$

and in terms of the generators of the subgroups given by Eq. (4) we have

$$Q_\psi=\sqrt{3/8}(Y_L-Y_R)\,, \tag{6a}$$

$$Q_\chi=\frac{1}{\sqrt{10}}[2I_{3R}-\tfrac{3}{2}(Y_L+Y_R)]\,, \tag{6b}$$

where we use the conventions given by Rosner in Ref. 5. To find Q'_η we note that the Z' must couple to a linear combination of Y_L and Y_R+2I_{3R} orthogonal to that appearing in the Z^0 charge, $I_{3R}+(Y_L+Y_R)/2$. Properly normalized we obtain

$$\begin{aligned}Q'_\eta&=\left[\frac{3}{5}\right]^{1/2}\left[\frac{1}{2}\left[I_{3R}+\frac{Y_R}{2}\right]-Y_L\right]\\&=-\left[\frac{5}{8}\right]^{1/2}Q_\psi+\left[\frac{3}{8}\right]^{1/2}Q_\chi\,.\end{aligned} \tag{7}$$

Thus, in this model, we find $\cos\theta_{E_6}=\sqrt{3/8}$ and $\sin\theta_{E_6}=-\sqrt{5/8}$.

We next consider the fermions in E_6 and their quantum numbers. Under the two maximal subgroups of E_6, $SU(3)_C\times SU(3)_L\times SU(3)_R$ and $SO(10)\times U(1)_\psi$, the fundamental 27-dimensional representation breaks to

$$\begin{aligned}&27\to(3,3,1)+(3^*,1,3^*)+(1,3^*,3)\,,\\&27\to(16,1)+(10,-2)+(1,4)\,,\end{aligned} \tag{8}$$

respectively. The 27 has 9 color singlets, 3 quarks, and 3 antiquarks where two quarks have electric charge $-\frac{1}{3}$ and the remaining quark has charge $+\frac{2}{3}$. Assuming that the 16 ordinary fermions of each generation (including the right-handed neutrino) belong to the **16** of SO(10), we can uniquely determine the quantum numbers of all fermions in the fundamental representation of E_6. The 11 new fermions include a new charge $-\frac{1}{3}$ quark, an isodoublet of charged and neutral leptons E^- and ν_E, and their antiparticles which form the **10** of SO(10), and an extra neutrino which is the SO(10) singlet. We list the fermions for one generation and their quantum numbers in Table I.

In terms of these fields the neutral-current Lagrangian can be written as

$$L_{\rm NC}=eA_\mu J^\mu_{\rm EM}+g_{Z^0}Z^0_\mu J^\mu_{Z^0}+g_{Z'}Z'_\mu J^\mu_{Z'}\,, \tag{9}$$

where $J^\mu_{\rm EM}$ and $J^\mu_{Z^0}$ are as in the standard model and

$$J^\mu_{Z'}=\sum_f \bar{\psi}_f\gamma^\mu(C'_V-C'_A\gamma_5)\psi_f \tag{10}$$

with $C'_{V,A}=(Q'_f\mp Q'_{\bar{f}})/2$. The values of Q'_f for the fermions are taken from the last three columns in Table I. For convenience we list in Table II C'_V and C'_A of the electron for some specific cases. We consider only the

TABLE II. Couplings of the e^-, μ^-, and τ^- to Z' for some representative θ_{E_6} directions. Here $\theta_\chi=0°$, $\theta_\psi=90°$, and θ_η is given by Eq. (7).

	C_L	C_R	C_V	C_A
θ_χ	$3/2\sqrt{10}$	$1/2\sqrt{10}$	$1/\sqrt{10}$	$1/2\sqrt{10}$
θ_ψ	$1/\sqrt{24}$	$-1/\sqrt{24}$	0	$1/\sqrt{24}$
θ_η	$1/2\sqrt{15}$	$+1/\sqrt{15}$	$3/4\sqrt{15}$	$-1/4\sqrt{15}$

minimal case of one extra neutral gauge boson assuming that in the case of rank-6 groups where two extra neutral bosons are present, one of them is sufficiently heavier than the other so that its effects are suppressed up to energies around the Z^0 mass. We therefore have four phenomenological parameters in the analysis: θ_{E_6}—the Q_χ-Q_ψ mixing angle, ϕ—the Z^0-Z' mixing angle, M_Z'—the mass of the extra Z^0 boson, and $(g_{Z'}/g_{Z^0})$—the ratio of the Z' and Z^0 coupling constants. This ratio, $(g_{Z'}/g_{Z^0})$, can be found in a specific symmetry-breaking scheme using the renormalization-group equations and is given by $(g_{Z'}/g_{Z^0})^2 \leq \frac{5}{3}\sin^2\theta_W$ (Ref. 10). It takes on its maximum value when the extra U(1) breaks off at the same scale as the breaking to $SU(3)_C \times SU(2)_L \times U(1)$ and we use the maximum value in what follows. The angle ϕ is related to the standard-model prediction for the mass of the Z^0 (M_{SM}), the observed M_{Z^0}, and $M_{Z'}$

$$\tan^2\phi = \frac{M_{SM}{}^2 - M_{Z^0}{}^2}{M_{Z'}{}^2 - M_{SM}{}^2} , \tag{11}$$

where $M_{SM} = M_W/\cos\theta_W$. With an accurate measurement of the physical Z^0 mass ϕ can be related to $M_{Z'}$ and can therefore be removed as a free parameter. This leaves θ_{E_6} and $M_{Z'}$ to be determined.

III. ASYMMETRIES FROM EXTRA Z^0's

Our goal is to study the effects of extra Z^0's on asymmetries in e^+e^- colliders and to unravel the underlying physics. With this in mind we will examine forward-backward asymmetries and left-right asymmetries in $e^+e^- \to \mu^+\mu^-$ and also asymmetries which can arise in Bhabha scattering. With efficient flavor tagging of heavy quarks in jets one could repeat the exercise for $e^+e^- \to q\bar{q}$.

We begin with the asymmetries in $e^+e^- \to \mu^+\mu^-$. The processes which contribute to the cross sections are given in Fig. 1. Evaluating the amplitudes of Fig. 1 one obtains for the cross section of an unpolarized positron and a left-handed polarized electron

$$\frac{d\sigma_L}{d\cos\theta} = \frac{\pi\alpha^2}{2s}[\,|b_{LL}|^2(1+\cos\theta)^2 + |b_{LR}|^2(1-\cos\theta)^2\,] , \tag{12}$$

where

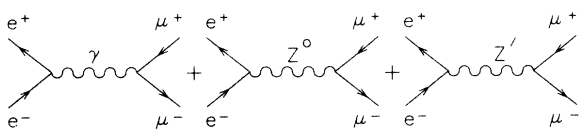

FIG. 1. Processes which contribute to the $e^+e^- \to \mu^+\mu^-$ cross section.

$$b_{ij} = 1 + \frac{C_i^e C_j^\mu}{4\cos^2\theta_W \sin^2\theta_W} \frac{s}{s - M_{Z^0}{}^2 + i\Gamma_{Z^0}M_{Z^0}} + \frac{(g_{Z'}/g_{Z^0})^2 C_i^{e'} C_j^{\mu'}}{4\cos^2\theta_W \sin^2\theta_W} \frac{s}{s - M_{Z'}{}^2 + i\Gamma_{Z'}M_{Z'}} , \tag{13}$$

and $i,j = L,R$. In these expressions $C_{L,R} = C_V \pm C_A$. For the cross section with a right-handed electron one makes the replacement $L \leftrightarrow R$. In our calculations we will use the values $\sin^2\theta_W = 0.222$, $M_{Z^0} = 92.5$ GeV, and $\Gamma_{Z^0} = 2.5$ GeV. The value of $\sin^2\theta_W$ was obtained by Barger, Deshpande, and Whisnant[6] from a fit to the low-energy neutral-current data for $\theta_{E_6} = \theta_\eta$ and includes radiative corrections. Durkin and Langacker[7] found that $\sin^2\theta_W$ was not very sensitive to the model used to fit the low-energy data (i.e., the value for θ_{E_6}) even when Z^0-Z' mixing effects were included. This is also the radiatively corrected standard model value obtained using[11]

$$\sin^2\theta_W \simeq \frac{1}{2}\left[1 - \left[1 - \frac{4\pi\alpha_{EM}}{\sqrt{2}G_\mu M_{Z^0}{}^2(1-0.06)}\right]^{1/2}\right] \tag{14}$$

with $G_\mu = 1.166\,37 \times 10^{-5}$ GeV^{-2} and $M_{Z^0} = 92.5$ GeV and where the factor 0.06 comes from the light-quark contributions to the vacuum polarization. The standard-model result remains valid when extra Z^0's are present if there is no mixing between Z^0 and Z' and only Higgs doublets and singlets contribute to the mass matrix. The Z' width is given by

$$\Gamma_{Z'} = \frac{g_{Z'}{}^2 M_{Z'}}{12\pi} \sum_f (C_V^{f'2} + C_A^{f'2}) . \tag{15}$$

To obtain a value for $\Gamma_{Z'}$ we included only the fermions of the first three generations of the standard model. If the extra fermions of E_6 were discovered their contribution to the width could be included. In any case our results are rather insensitive to the exact value of the Z' width.

We have not included detector-dependent radiative corrections such as bremsstrahlung off the initial or final legs and virtual-photon graphs in our calculations.[12] This is because the corrections from the soft bremsstrahlung and virtual-photon diagrams depend on the detector resolution ΔE and those from the hard bremsstrahlung graphs depend crucially on the experimental acceptance cuts and can be large, up to 30% of the tree-level contributions. These are best included by experimentalists via Monte Carlo simulations involving the details of their detectors.[11]

A. Left-right asymmetry

The left-right asymmetry A_{LR} is defined by

$$A_{LR} = \frac{\sigma_L - \sigma_R}{\sigma_L + \sigma_R} . \tag{16}$$

In what follows we will display our results as the difference between the asymmetry with an extra Z^0 and that of the standard model: i.e.,

$$\delta A_{LR} = A_{LR} - A_{LR}(\mathrm{SM}) .$$

In Fig. 2 we plot δA_{LR} at $\sqrt{s}=100$ GeV as a function of θ_{E_6}. We have set the Z^0-Z' mixing angle to zero. In Fig. 3 we show δA_{LR} as a function of $\sqrt{s}$ for the specific value of θ_η which arises in some superstring theories and for several values of $M_{Z'}$. Not unexpectedly the larger the $\sqrt{s}$ and the lower the Z' mass the larger the deviation from the standard model. Also, without Z^0-Z' mixing the deviation at the Z^0 pole is negligible which simply reflects the dominance of the Z^0 pole. Much below the Z^0 pole, δA_{LR} is dominated by the γ-Z' interference term and is proportional to $C_V'C_A'$. However, as $\sqrt{s}$ increases the Z^0-Z' interference takes over and the dependence on $C_{V,A}$ and $C'_{V,A}$ is more complicated. We will return to this issue in the discussion.

Finally, in Fig. 4 we consider the effect of Z^0-Z' mixing. We use the allowed bounds on Z^0-Z' mixing and $M_{Z'}$ obtained from the analysis of low-energy data by Durkin and Langacker.[7] One sees that for the amount of mixing allowed by low-energy phenomenology, the deviations from the standard model in the left-right asymmetry can be quite substantial. In fact, the Z^0-Z' mixing will be the dominant effect on asymmetries. The reason for this is that the Z^0 coupling is modified by the Z', i.e.,

$$C_V \rightarrow C_V \cos\phi + C_V' \sin\phi \ .$$

The C_V' and C_A' terms are suppressed only by a mixing angle, not by a factor of $1/M_{Z'}^2$ as in the absence of mixing. The effects are therefore particularly significant around the Z^0 pole.[13]

B. Front-back asymmetry

The front-back asymmetry A_{FB} is defined by

$$A_{FB}=\frac{\int_0^1 d\cos\theta \frac{d\sigma}{d\cos\theta} - \int_{-1}^0 d\cos\theta \frac{d\sigma}{d\cos\theta}}{\int_0^1 d\cos\theta \frac{d\sigma}{d\cos\theta} + \int_{-1}^0 d\cos\theta \frac{d\sigma}{d\cos\theta}} \qquad (17)$$

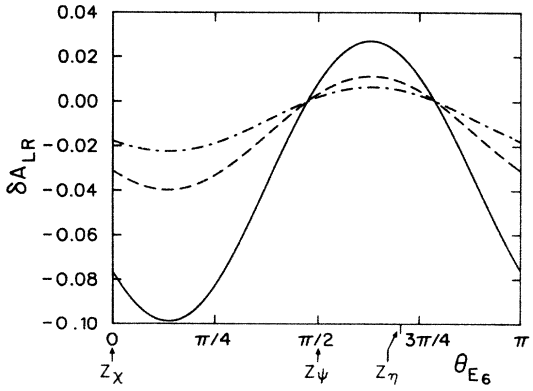

FIG. 2. δA_{LR} as a function of θ_{E_6}. The solid curve is for $M_{Z'}=150$ GeV, the dashed curve for $M_{Z'}=200$ GeV, and the dot-dashed curve for $M_{Z'}=250$ GeV. In all cases $\sqrt{s}=100$ GeV and $\phi=0$. We point out the special angles corresponding to Z_χ, Z_ψ, and Z_η. For Z_η we actually show $\theta_\eta+\pi$ which corresponds to the same asymmetry as θ_η.

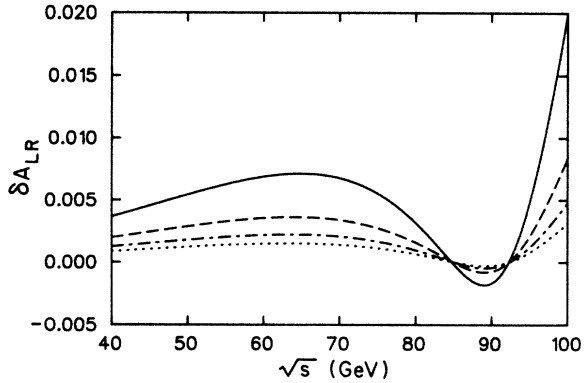

FIG. 3. δA_{LR} as a function of $\sqrt{s}$ for several values of M_Z' with $\theta_{E_6}=\theta_\eta$ and $\phi=0$. The solid curve is for $M_{Z'}=150$ GeV, the dashed curve for $M_{Z'}=200$ GeV, the dash-dotted curve for $M_{Z'}=250$ GeV, and the dotted curve for $M_{Z'}=300$ GeV.

and $\delta A_{FB}=A_{FB}-A_{FB}(\mathrm{SM})$.

In Fig. 5(a) we show δA_{FB} as a function of θ_{E_6} for $\sqrt{s}=100$ GeV for left-polarized, right-polarized, and unpolarized electrons, illustrating the effect of polarized beams on front-back asymmetries, and in Fig. 5(b) we show the effect of varying the Z' mass. In Fig. 6 we show δA_{FB} as a function of $\sqrt{s}$ for $\theta_{E_6}=\theta_\eta$ for several values of $M_{Z'}$. Examining the expression for A_{FB} we find that much below the Z^0 peak δA_{FB} is dominated by the γ-Z' interference term and is proportional to $C_A'^2$. Around the Z^0 peak the Z^0-Z' term dominates and is approximately proportional to $C_A^2 C_V'^2$. Again, in Fig. 7, we show some representative deviations of A_{FB} from the standard model for values of the parameters allowed by low-energy phenomenology and once again they are found to be quite substantial.

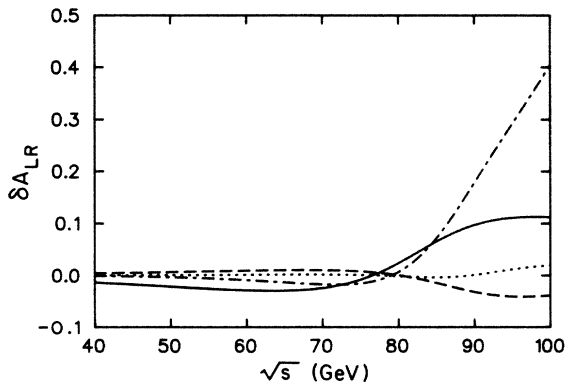

FIG. 4. δA_{LR} vs $\sqrt{s}$ for some representative parameter sets allowed by current data. The solid curve is for Z_χ with $M_{Z'}=260$ GeV and $\phi=-0.08$, the dot-dashed line is for Z_η with $M_{Z'}=120$ GeV and $\phi=-0.25$, the dashed line for Z_η with $M_{Z'}=200$ GeV and $\phi=+0.04$, and the dotted line is for Z_ψ with $M_{Z'}=140$ GeV and $\phi=+0.06$.

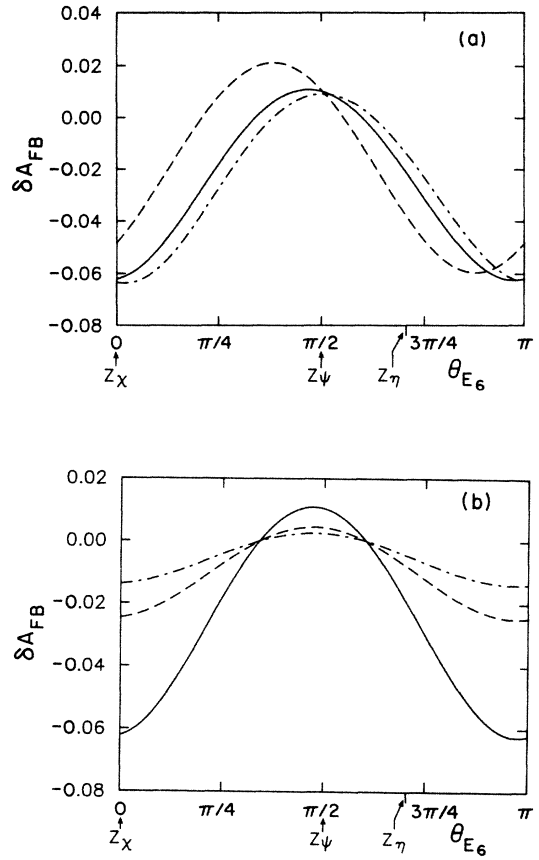

FIG. 5. δA_{FB} as a function of θ_{E_6} for $\sqrt{s}=100$ GeV. In (a) we take $M_{Z'}=150$ GeV and $\phi=0$. The solid line is for unpolarized electrons, the dashed line is for a right-polarized beam, and the dot-dashed line is for a left-polarized electron beam. In (b) we vary $M_{Z'}$ for an unpolarized electron beam. The solid line is for $M_{Z'}=150$ GeV, the dashed line for $M_{Z'}=200$ GeV, and the dot-dashed line for $M_{Z'}=250$ GeV.

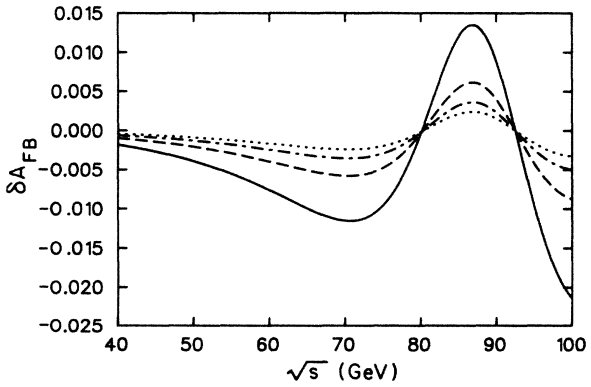

FIG. 6. δA_{FB} vs $\sqrt{s}$ for an unpolarized electron beam and $\theta_{E_6}=\theta_\eta$ and $\phi=0$. The solid line is for $M_{Z'}=150$ GeV, the dashed line for $M_{Z'}=200$ GeV, the dot-dashed line for $M_{Z'}=250$ GeV, and the dotted line for $M_{Z'}=300$ GeV.

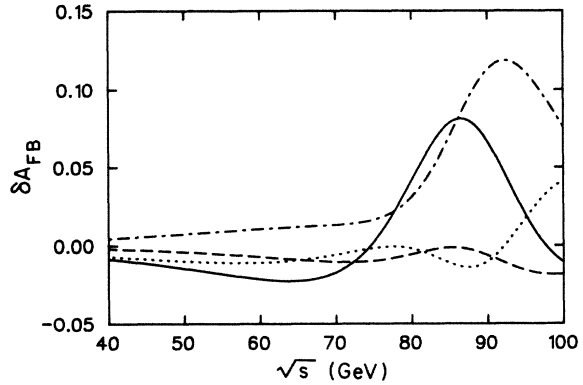

FIG. 7. δA_{FB} vs $\sqrt{s}$ with unpolarized electrons for some representative parameter sets allowed by current data. The solid curve is for Z_χ with $M_{Z'}=260$ GeV and $\phi=-0.08$, the dot-dashed line is for Z_η with $M_{Z'}=120$ GeV and $\phi=-0.25$, the dashed line for Z_η with $M_{Z'}=200$ GeV and $\phi=+0.04$, and the dotted line is for Z_ψ with $M_{Z'}=140$ GeV and $\phi=+0.06$.

C. Bhabha scattering

For the final example we consider the effect of extra Z^0's on Bhabha scattering. In addition to the s-channel diagram of Fig. 1 we must also include the t-channel diagrams of Fig. 8. Including these t-channel diagrams in the amplitude leads to the differential cross section

$$\frac{d\sigma_L}{d\cos\theta}=\frac{\pi\alpha^2}{2s}[\,|\,b_{LL}+d_{LL}\,|^2(1+\cos\theta)^2 + |\,b_{LR}\,|^2(1-\cos\theta)^2+4\,|\,d_{LR}\,|^2] \tag{18}$$

with the b_{ij}'s defined as in Eq. (13) and with the d_{ij}'s defined by

$$d_{ij}=1+\frac{C_i^eC_j^e}{4\cos^2\theta_W\sin^2\theta_W}\frac{t}{(t-M_{Z^0}{}^2)+i\Gamma_{Z^0}M_{Z^0}} + \frac{(g_{Z^0}/g_{Z'})^2C_i^{e'}C_j^{e'}}{4\cos^2\theta_W\sin^2\theta_W}\frac{t}{(t-M_{Z'}{}^2)+i\Gamma_{Z'}M_{Z'}} \tag{19}$$

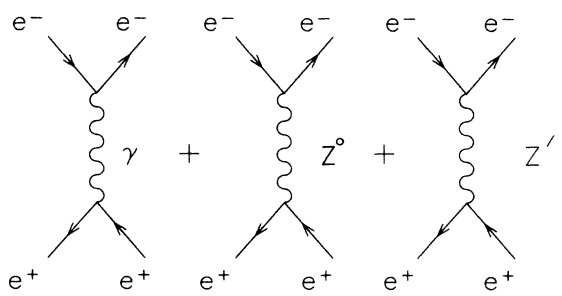

FIG. 8. The t-channel processes, in addition to the s-channel processes of Fig. 1, which contribute to the $e^+e^-\to e^+e^-$ Bhabha scattering cross section.

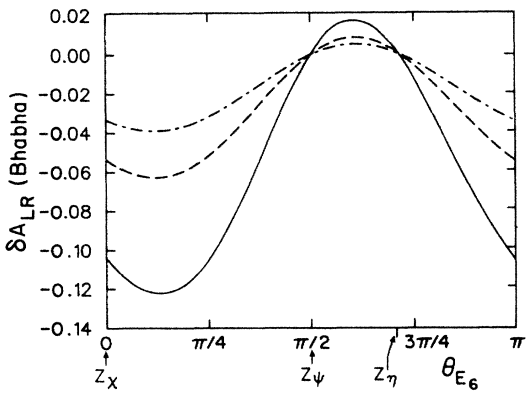

FIG. 9. δA_{LR} (Bhabha) vs θ_{E_6} for $\sqrt{s}=100$ GeV and for the e^- polar scattering angle $\theta=90°$. The solid line is for $M_{Z'}=150$ GeV, the dashed line for $M_{Z'}=200$ GeV, and the dot-dashed line for $M_{Z'}=250$ GeV.

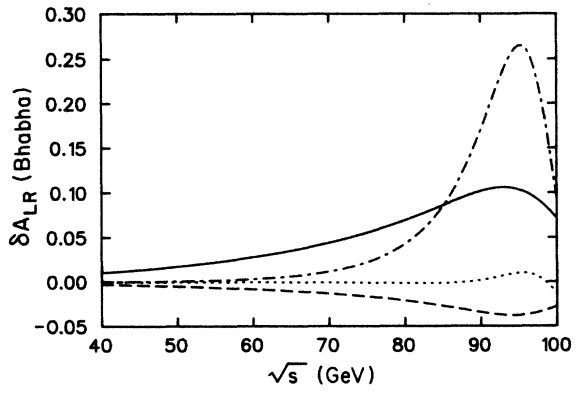

FIG. 11. δA_{LR} (Bhabha) vs $\sqrt{s}$ for some representative parameter sets allowed by current data. The line labeling is as in Fig. 7.

with $i,j=L,R$. For the cross section with right-polarized electrons make the substitution $L\leftrightarrow R$. From this expression we can define a left-right asymmetry as before. However, instead of integrating over all θ we take $d\sigma/d\cos\theta$ at $\theta=90°$ to minimize the effects of the photon pole in the t channel and maximize the effects of the extra Z^0 boson. Figure 9 illustrates the variation of δA_{LR} (Bhabha) as a function of θ_{E_6} for $\sqrt{s}=100$ GeV and several values of $M_{Z'}$ and Fig. 10 shows how δA_{LR} (Bhabha) varies with $\sqrt{s}$ for $\theta_{E_6}=\theta_\eta$. Once again, in Fig. 11, we see that the allowed deviations from the standard model are quite considerable when there is mixing between the Z^0 and Z'.

IV. DISCUSSION AND CONCLUSIONS

As can be seen from the various figures, the asymmetries due to an extra Z^0 boson can deviate quite substantially from that of the standard model. One can obtain relations between the asymmetries and $M_{Z'}$, C_V', and C_A' but in general it is nontrivial to extract the parameters of the model from the expression for the various asymmetries. An alternate method, while not as direct, is to make a contour plot of the δA's as a function of θ_{E_6} and $M_{Z'}$. Since δA_{LR}, δA_{FB}, and δA_{LR} (Bhabha) have different functional dependencies on θ_{E_6}, $M_{Z'}$, and $\sqrt{s}$, by measuring the asymmetries one can constrain the allowed region of the parameter space. If deviations are found the measured values would restrict the properties of the Z' to a region of the θ_{E_6}-$M_{Z'}$ plane. We illustrate this method in Fig. 12 where we have plotted contours of constant δA_{LR}, δA_{FB}, and δA_{LR} (Bhabha) for $\sqrt{s}=100$ GeV. Depending on flavor-tagging efficiencies one could also utilize asymmetries involving $c\bar{c}$ and $b\bar{b}$ pairs in the final

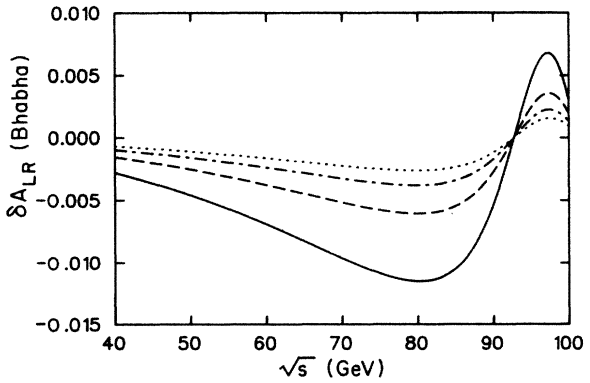

FIG. 10. δA_{LR} (Bhabha) vs $\sqrt{s}$ for $\theta_{E_6}=\theta_\eta$ and the e^- polar scattering angle $\theta=90°$. The solid line is for $M_{Z'}=150$ GeV, the dashed line for $M_{Z'}=200$ GeV, the dot-dash line for $M_{Z'}=250$ GeV, and the dotted line for $M_{Z'}=300$ GeV.

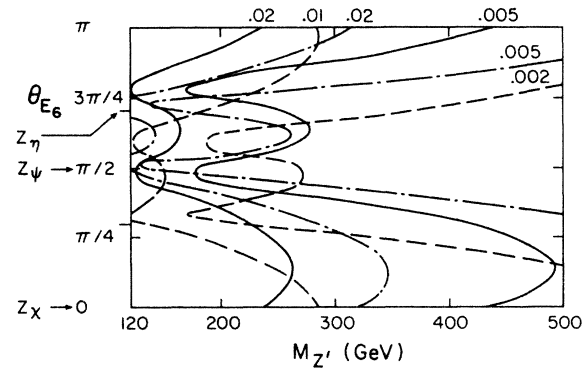

FIG. 12. Contour plot of deviations from the standard model for the various asymmetries in the θ_{E_6}-$M_{Z'}$ plane. The solid lines are for δA_{LR}, the dashed lines for δA_{FB}, and the dot-dashed line for δA_{LR} (Bhabha). All are for $\sqrt{s}=100$ GeV and $\phi=0$.

state. Because the quarks will in general have different couplings to the Z' than the leptons, shifts in the asymmetries which differ from those involving leptons would help unravel the underlying theory.

To conclude, we have studied the asymmetries in e^+e^- colliders that may arise from E_6 GUT's and have found that asymmetries provide a sensitive probe of new physics. In fact, the deviations in asymmetries from the standard model allowed by current data are quite substantial and accurate measurements would severely restrict models proposed for new physics. Asymmetries measured at e^+e^- colliders could very well be our first indication of new physics beyond the standard model.

Note added in proof. After the submission of this paper we became aware of several related papers[14–17] to which we refer the interested reader.

ACKNOWLEDGMENTS

We are most grateful to David London and John Ng for on-going discussions and numerous suggestions during the course of this work. This work was partially funded by the Natural Science and Engineering Research Council of Canada.

[1]E. Witten, Phys. Lett. **155B**, 1551 (1985); Nucl. Phys. **B258**, 75 (1985); P. Candelas, G. T. Horowitz, A. Strominger, and E. Witten, *ibid.* **B258**, 46 (1985).

[2]M. Dine *et al.*, Nucl. Phys. **B259**, 549 (1985).

[3]J. D. Breit, B. A. Ovrut, and G. C. Segrè, Phys. Lett. **158B**, 33 (1985); S. Cecotti *et al.*, *ibid.* **156B**, 318 (1985); P. Kalyniak and M. K. Sundaresan, *ibid.* **167**, 320 (1986); J. L. Hewett, T. G. Rizzo, and J. A. Robinson, Phys. Rev. D **33**, 1476 (1986); P. K. Mohapatra, R. N. Mohapatra, and P. B. Pal, *ibid.* **33**, 2010 (1986).

[4]R. W. Robinett, Phys. Rev. D **33**, 1908 (1986); V. Barger, N. Deshpande, R. J. N. Phillips, and K. Whisnant, *ibid.* **33**, 1912 (1986).

[5]J. Rosner, Comments Nucl. Part. Phys. **15**, 195 (1986).

[6]V. Barger, N. G. Deshpande, and K. Whisnant, Phys. Rev. Lett. **56**, 30 (1986); S. M. Barr, *ibid.* **55**, 2778 (1985); E. Cohen, J. Ellis, K. Enqvist, and D. V. Nanopoulos, Phys. Lett. **165B**, 76 (1985).

[7]L. S. Durkin and P. Langacker, Phys. Lett. **166B**, 436 (1986).

[8]For earlier work see W. Hollik, Z. Phys. C **8**, 149 (1981) and references therein.

[9]For a review of the relevant group theory see, for instance, R. Slansky, Phys. Rep. **79**, 1 (1981).

[10]See, for instance, R. W. Robinett, Phys. Rev. D **26**, 2388 (1982); R. W. Robinett and J. L. Rosner, *ibid.* **25**, 3036 (1982); **26**, 2396 (1982) and references therein.

[11]B. W. Lynn, M. E. Peskin, and R. G. Stuart, in *Physics at LEP*, edited by J. Ellis and R. Peccei (CERN Report No. 86-02, 1986); B. W. Lynn and R. G. Stuart, Nucl. Phys. **B253**, 216 (1985).

[12]M. Bohm and W. Hollik, Nucl. Phys. **B204**, 45 (1982); M. Greco, G. Pancheri-Srivastava, and Y. Strivastava, *ibid.* **B171**, 118 (1980); R. Berends and P. Kleiss, *ibid.* **B177**, 237 (1981).

[13]S. Godfrey and G. Bélanger, TRIUMF Report No. TRI-PP-86-18, 1986 (unpublished).

[14]P. J. Franzini, Report No. SLAC-PUB-3920, 1986 (unpublished); P. J. Franzini and F. J. Gilman, Report No. SLAC-PUB-3932, 1986 (unpublished).

[15]V. D. Angelopoulos, J. Ellis, and D. V. Nanopoulos, Report No. CERN-TH.4408/86, 1986 (unpublished).

[16]T. G. Rizzo, Ames Laboratory Report No. IS-J2167, 1986 (unpublished).

[17]M. Cvetič and B. W. Lynn, Report No. SLAC-PUB-3900, 1986 (unpublished).